Eya1 and Six1 are essential for early steps of sensory neurogenesis in mammalian cranial placodes

Dan Zou[1], **Derek Silvius**[1], **Bernd Fritzsch**[2], and **Pin-Xian Xu**[1,*]

[1]McLaughlin Research Institute for Biomedical Sciences, 1520 23rd Street South, Great Falls, MT 59405, USA

[2]Department of Biomedical Sciences, Creighton University, 2500 California Plaza, Omaha, NE 68178, USA

Summary

Eya1 encodes a transcriptional co-activator and is expressed in cranial sensory placodes. It interacts with and functions upstream of the homeobox gene *Six1* during otic placodal development. Here, we have examined their role in cranial sensory neurogenesis. Our data show that the initial cell fate determination for the vestibuloacoustic neurons and their delamination appeared to be unaffected in the absence of Eya1 or Six1 as judged by the expression of the basic helix-loop-helix genes, *Neurog1* that specifies the neuroblast cell lineage, and *Neurod* that controls neuronal differentiation and survival. However, both genes are necessary for normal maintenance of neurogenesis. During the development of epibranchial placode-derived distal cranial sensory ganglia, while the phenotype appears less severe in *Six1* than in *Eya1* mutants, an early arrest of neurogenesis was observed in the mutants. The mutant epibranchial progenitor cells fail to express *Neurog2* that is required for the determination of neuronal precursors, and other basic helix-loop-helix as well as the paired homeobox *Phox2* genes that are essential for neural differentiation and maintenance. Failure to activate their normal differentiation program resulted in abnormal apoptosis of the progenitor cells. Furthermore, we show that disruption of viable ganglion formation leads to pathfinding errors of branchial motoneurons. Finally, our results suggest that the Eya-Six regulatory hierarchy also operates in the epibranchial placodal development. These findings uncover an essential function for Eya1 and Six1 as critical determination factors in acquiring both neuronal fate and neuronal subtype identity from epibranchial placodal progenitors. These analyses define a specific role for both genes in early differentiation and survival of the placodally derived cranial sensory neurons.

Keywords

Eya1; Six1; Otic; Epibranchial; Placode; Sensory neurons; Neurogenesis; Neurogenins; bHLH protein; Phox2a; Phox2b; Cranial nerve patterning

Introduction

In vertebrates, all peripheral sensory neurons derive either from precursors in placodes or from neural crest cells. Placodes are focal regions of thickened ectoderm in the vertebrate head, which give rise to both neuronal and non-neuronal structures (the lens of the eye and the anterior pituitary) (Le Douarin, 1984). The neurogenic placodes include the olfactory, otic, trigeminal, and epibranchial placodes. Of these, only the olfactory and otic placodes

---

*Author for correspondence (pxu@po.mri.montana.edu).

give rise to neuronal and non-neuronal components, while the trigeminal and epibranchial placodes generate exclusively sensory neurons of the trigeminal (V) and the distal geniculate (VII), petrosal (IX) and nodose (X) ganglia. The facial (VIIth), glossopharyngeal (IXth), and vagal (Xth) cranial nerves also have associated proximal facial (VII), jugular (IX), and superior (X) ganglia, which are of neural crest origin (Ayer-Le Lievre and Le Douarin, 1982; D'Amico-Martel and Noden, 1983), and fibers of branchiomotor and visceromotor origin (Fritzsch and Northcutt 1993; Ma et al., 2000). Although the ontogenies of sensory neurons within those cranial ganglia have been well described, how the placodal ectodermal cells are induced to differentiate into neuronal cells, and the molecular mechanisms that direct their development along this pathway are not well established.

Targeted mutagenesis in mice has shown that the basic helix-loop-helix (bHLH) transcription factor neurogenins (Neurogs) play a critical role in early development of the placodally derived cranial sensory neurons. Neurog1 and Neurog2 are expressed in the cranial placodes as early as E8.5 and act as critical determination factors for cell fate commitment (Fode et al., 1998; Ma et al., 1998; Ma et al., 1999; Ma et al., 2000). While Neurog1 is required for the formation of the V and VIII sensory neurons (Ma et al., 1998), Neurog2 is necessary for normal development of the epibranchial placode-derived sensory neurons of VII, IX and X (Fode et al., 1998). Recent studies have found that Neurogs may activate a cascade of downstream bHLH factors, including Math3, Neurod and Nscl1, to promote the development of the placode-derived sensory neurons (Fode et al., 1998; Ma et al., 1998). Neurogs are necessary for normal expression of these factors, but it is unclear whether all these genes act in a linear pathway and none of them has been proven to be a direct target of Neurog1 or Neurog2.

The epibranchial placode-derived sensory neurons of the distal VII, IX, and X ganglia also depend on the paired homeodomain transcription factors Phox2a and Phox2b for their differentiation and survival. *Phox2a* has been shown to function upstream of *Phox2b* (Pattyn et al., 1999) and in *Phox2a*$^{-/-}$ and *Phox2b*$^{-/-}$ mice, epibranchial placodes give rise to the normal number of neuroblasts, but these neuroblasts fail to activate their more specific differentiation program (Morin et al., 1997; Pattyn et al., 1999; Pattyn et al., 2000). Epibranchial placodal sensory precursors require Phox2a for a subprogram of neuron-subtype-specific gene expression that can be genetically independent from a subprogram for pan-neuronal gene expression, which requires Neurog2 function (Fode et al., 1998). However, details of the *Neurogs* and *Phox2* genes' mode of action in neuronal cells have not been elucidated.

The murine Eya gene family, homologous to *eyes absent* (*eya*), which is required for normal eye development in *Drosophila* (Bonini et al., 1993), is composed of four members (*Eya1–4*) and encodes a transcriptional co-activator containing a conserved C-terminal Eya domain involved in protein-protein interaction, and a divergent N-terminal transactivation domain (Xu et al., 1997a; Xu et al., 1997b; Borsani et al., 1999). The conserved Eya domain of Eya proteins interacts with Sine oculis (So) or Dachshund (Dach), other regulators for *Drosophila* eye development (Chen et al., 1997; Pignoni et al., 1997). *Eya1* genes are expressed in multiple domains including many ectodermal placodes and this expression pattern appears to be conserved from *Xenopus* and zebrafish to mammals (Xu et al., 1997a; Sahly et al., 1999; David et al., 2001; Schlosser and Ahrens, 2004). Among the cranial placodes, *Eya1* has been shown to play an essential role in otic placode development (Xu et al., 1999; Zheng et al., 2003). *Six1*, a member of the Six gene family homologous to *Drosophila so*, encodes a homeodomain protein and its gene product physically interacts with Eya1 (Buller et al., 2001). During otic placodal development, *Six1* functions downstream of and genetically interacts with *Eya1* (Zheng et al., 2003). Interestingly, *Six1*-deficient mice show defects in all three parts of the ear similar to that observed in *Eya1*

mutants (Xu et al., 1999; Zheng et al., 2003). However, it is unknown whether Eya1 and Six1 play a role in the generation of otic and other placode-derived sensory neurons.

Placodal and neural crest-derived ganglia appear to be necessary for trigeminal branchial motoneurons to exit the brain (Moody and Heaton, 1983; Ma et al., 2000). Absence or lack of differentiation of all VII and VIII ganglia (Zheng et al., 2003) may not only alter the trajectory of inner ear efferents into the facial nerve (Ma et al., 2000), but may cause redirection of facial branchial motoneuron fibers into still existing cranial nerves. *Eya1-* and *Six1*-null mutants could therefore provide a test for the hypothesis that all branchial motoneurons require sensory neuron fibers to grow along to the peripheral nerves (Fritzsch and Northcutt, 1993).

In this study, we address whether Eya1 and Six1 are required for specific placodal precursor specification, survival and differentiation, and for branchial motoneurons exiting from the brainstem. We found that in addition to affecting VIII ganglion formation, these genes control epibranchial placode neurogenesis. During inner ear neurogenesis, Eya1 and Six1 appear to be dispensable for the initiation of neurogenesis, but both may regulate the progressive differentiation of neuroblast precursor cells. Strikingly, in contrast, the mutant epibranchial placodal progenitor cells fail to express both neuronal fate and neuronal subtype identity of the epibranchial placode-derived sensory lineage due to defective expression of *Neurog2* and *Phox2a*. Shortly thereafter, increased cell death is detected in the mutant placodal ectoderm, suggesting that in the absence of their normal developmental program, the placodal progenitor cells undergo apoptosis. Moreover, whole-mount staining with the neuroglial marker *Sox10* and neurofilament antibody at E10.5, and retrograde as well as anterograde labeling of motor neurons at E13.5 indicated that both Eya1 and Six1 regulate the proper routing of facial branchial motoneurons. Together, our analyses establish that Eya1 functions upstream of Six1 and both act as critical determination factors for epibranchial placodal progenitor cells to acquire both neural fate and subtype sensory identity.

Materials and methods

Animals and genotyping

Eya1- and *Six1*-null mice were generated as reported (Xu et al., 1999; Laclef et al., 2003). Genotyping of mice and embryos was performed as described (Xu et al., 1999; Xu et al., 2002).

Phenotype analyses and in situ hybridization

Embryos for histology and in situ hybridization were dissected out in PBS and fixed with 4% paraformaldehyde (PFA) at 4°C overnight. Embryonic membranes were saved in DNA isolation buffer for genotyping. For whole-mount and section in situ hybridization, we used 4–6 wild-type or mutant embryos at each stage for each probe as described (Xu et al., 1997a).

Antibody staining and neuronal tract tracing

Whole-mount immunostaining using the anti-neurofilament monoclonal antibody 2H3 (Developmental Studies Hybridoma Bank) was performed as described (Mark et al., 1993).

For neuronal tracing, E13.5 embryos were dissected, fixed in 4% PFA and labeled using fast diffusion of lipophilic dyes as described previously (Maklad and Fritzsch, 2003a). Embryos were dissected and the dye-filled profiles were viewed with a BioRad 2000 confocal microscope.

Results

Common phenotype in neurogenesis of *Eya1*$^{-/-}$ and *Six1*$^{-/-}$ mutant inner ears

The embryonic VIIIth ganglion consists of a mixture of neurons and neuroblasts, with a common origin from neuroblasts in the otic ectoderm (Adam et al., 1998; Farinas et al., 2001). The neuroblast precursors are the first cell lineage specified within the otic ectoderm before leaving it, and *Neurog1* was found to be required for the formation of all VIII sensory neurons (Ma et al., 1998; Ma et al., 2000). We have previously reported that *Eya1*- and *Six1*-null mutants lacked the VIIIth ganglion in older embryos (Xu et al., 1999; Zheng et al., 2003). However, it is unknown whether the neuroblast cell lineage is specified in the absence of Eya1 or Six1. To determine the stages in neurogenesis of the inner ear affected by the *Eya1* or *Six1* mutation, we first analyzed the expression of *Neurog1*, an early marker of neurogenesis, in both mutant embryos from E8.5 to 10.5. *Neurog1* is expressed in the neuroblast precursors in ventral otic cup at E9.0 and its expression expands as otic development proceeds (Fig. 1A,D,G,J). *Neurog1* expression was also detected in the migrating precursors to form the VIIIth ganglion in normal embryos (data not shown, see Fig. 4A). In all *Eya1*$^{-/-}$ or *Six1*$^{-/-}$ mutant embryos (four for each mutant at each stage), *Neurog1* expression was almost unaffected at E9.0 before the otic vesicle is completely closed (Fig. 1B,C), indicating that neurogenesis is initiated normally in both mutants. However, *Neurog1* expression in the mutant otic vesicle was markedly reduced from E9.25, and by E10.5, only a few *Neurog1*-expressing cells were detected in the ventral otic vesicle in both mutants (Fig. 1E,F,H,I,K,L). In addition, a few patches of *Neurog1*-positive cells migrating away from the otic vesicle were also observed in the mutants (data not shown, see Fig. 4B,C), suggesting that the neuroblast precursors specified in the mutant otic ectoderm are able to delaminate for the formation of the VIIIth ganglion.

To further confirm this observation, we analyzed *Neurod* expression in the mutant embryos. Neurod is a potent neuronal differentiation factor and functions downstream of Neurog1 in the formation of VIII sensory neurons (Lee et al., 1995, Ma et al., 1998). In contrast to *Neurog1*$^{-/-}$ mutants, where a complete loss of sensory neurons is observed (Ma et al., 1998; Ma et al., 2000), some sensory neurons still remain in the inner ear of *Neurod*$^{-/-}$ mice (Kim et al., 2001). In E9.5 normal embryos, *Neurod* is strongly expressed in the cells within the otic vesicle and in the migratory cells, to form sensory neurons of the VIIIth ganglion (Fig. 1M). In all four E9.5 mutant embryos, although the number of *Neurod*-positive cells was significantly reduced, its expression both within the otic vesicle and in the cells migrating away from it was detected (Fig. 1N,O), confirming that the neuroblast cells are induced to differentiate into sensory neurons in the absence of Eya1 or Six1. Nonetheless, our results clearly demonstrate that Eya1 and Six1 are necessary for sensory neuron maintenance, probably by regulating neuronal differentiation.

Degeneration of neuroblasts in the developing VIIIth ganglion in *Eya1* and *Six1* mutants

Because we failed to detect the VIIIth ganglion in older *Eya1*$^{-/-}$ and *Six1*$^{-/-}$ embryos at its normal location on histological sections, it is possible that neuroblast cells observed in the younger mutant embryos degenerate and thus fail to form a morphologically detectable ganglion. We therefore sought to determine whether the neuroblasts in the developing VIIIth ganglion undergo abnormal cell death in the mutants. Transverse sections of E8.5 to 9.5 normal and mutant embryos were processed for the TUNEL detection method of apoptotic nuclei. Cell death in the VIIIth ganglion anlage in *Eya1*$^{-/-}$ and *Six1*$^{-/-}$ embryos was first observed at around E9.25 and became apparent by E9.5 in both mutants (arrow, Fig. 1Q,R), whereas very few apoptotic cells were seen in the controls (Fig. 1P). Thus, the defective formation of the VIIIth ganglion can be attributed, at least in part, to increased cell death.

Distinct phenotype in the distal cranial ganglia between *Eya1* and *Six1* mutant mice

To determine whether the formation of other cranial sensory ganglia is also affected in the mutants, we performed whole-mount staining with *SCG10*, an early marker of differentiating neurons, to label the cranial sensory ganglia. At E10.5, *SCG10* expression in the Vth, VIIIth and distal VIIth, IXth, and Xth ganglia was readily visible in normal embryos (Fig. 2A). However, *Eya1*$^{-/-}$ and *Six1*$^{-/-}$ mutant precursors in the forming VIIIth ganglion anlage failed to express *SCG10* (Fig. 2B,C). Strikingly, *Eya1*$^{-/-}$ embryos also lacked *SCG10* expression in the epibranchial placode-derived ganglia (Fig. 2B), whereas its expression was present in the *Eya1*$^{-/-}$ Vth ganglion with slight reduction. Similarly, *SCG10* staining was visible in the *Six1*$^{-/-}$ Vth ganglion, but was undetectable in the *Six1*$^{-/-}$ VIIth, and reduced in the IXth and Xth ganglia of all six embryos analyzed (Fig. 2C). These results indicate that in addition to the defective formation of the VIIIth ganglion in *Eya1* and *Six1* mutants, the formation of epibranchial placode-derived ganglia, which are specified by the bHLH transcription factor Neurog2, also requires Eya1 and Six1 function. The lack of expression of the early neural differentiation marker *SCG10* in the mutant embryos suggests that *Eya1* and *Six1* are required for overt neural differentiation of the precursors of cranial sensory ganglia in E9.5 to 10.5 embryos. These data demonstrate that Eya1 is essential for the formation of all epibranchial placode-derived distal ganglia, while Six1 may regulate the formation of subsets of the sensory neurons.

Neurogenesis in the epibranchial placodes is not initiated in *Eya1*$^{-/-}$ and is reduced in *Six1*$^{-/-}$ embryos

The epibranchial placodes are transient ectodermal thickenings present in the mouse embryo between approximately E8.5 and 10.5 of development. During this period, the ectodermal cells within these placodes become columnar and mitotically active, and are thought to generate neuroblasts or immature neurons, which delaminate from the placodes, migrate dorsomedially, and aggregate to form the distal ganglion anlagen. To determine the earliest stages in neurogenesis affected by the *Eya1* or *Six1* mutation, we analyzed the expression of early marker bHLH genes for neurogenesis in the epibranchial placodes. In mice, placodal neuronal precursors first express *Neurog2* (Fig. 2D), then delaminate and start expressing *Neurog1*, *Neurod, Math3* and *Nscl1* as they accumulate close to their site of aggregation. Recent studies have demonstrated that inactivation of *Neurog2* blocks the delamination of neuronal precursors from the placodes and abolishes their pan-neuronal fate in early-stage embryos (Fode et al., 1998). To our surprise, *Eya1*$^{-/-}$ embryos lacked *Neurog2* expression in all epibranchial placodes at E9.5–10.0 (Fig. 2E). In contrast to *Eya1* mutants, *Six1*$^{-/-}$ embryos exhibited variable phenotype in the VIIth precursors. Among the six E9.5–10.0 *Six1*$^{-/-}$ embryos stained with *Neurog2*, only two showed *Neurog2*-staining in very few cells in the VIIth precursors unilaterally (data not shown), and the others completely lacked *Neurog2* expression (Fig. 2F). In the IXth and Xth precursors, *Neurog2* expression was present in all six embryos analyzed but was markedly reduced in the IXth and less affected in the Xth precursors (Fig. 2F).

As all *Eya1*$^{-/-}$ embryos at E9.5–10.0 lacked *Neurog2* expression, we sought to determine the onset of the developmental arrest by examining *Neurog2* expression at earlier stages, from E8.5 to 9.5 using section in situ hybridization. *Neurog2* expression was strongly detected in the epibranchial placodes (Fig. 2G,J,M). Strikingly, no *Neurog2* expression was detected in these structures of *Eya1*$^{-/-}$ embryos at these stages (Fig. 2H,K,N), differing from the obvious *Neurog1* expression in the otic ectoderm. In all three *Six1*$^{-/-}$ embryos, only residual *Neurog2* expression was observed in the VIIth precursors (Fig. 2I), and its expression was also reduced in the IXth but was relatively normal in Xth precursors (Fig. 2I,L,O), similar to that observed by whole-mount staining (Fig. 2F). This result suggests that the activation of *Neurog2* expression in epibranchial placodes requires Eya1 function.

Since deletion of *Neurog2* results in a transient loss of neural fate in distal VII and IX ganglia at early stages, and the development of these ganglia appears to recover at later stages in *Neurog2*^{−/−} animals, probably due to functional compensation by *Neurog1* (Fode et al., 1998; Ma et al., 1998; Ma et al., 1999), we therefore analyzed the other neuronal bHLH genes in the mutant embryos at E9.5 to 10.5 to further define the developmental failure in *Eya1* and *Six1* mutant epibranchial placodes. Transcripts for *Neurog1*, which is weakly coexpressed with *Neurog2* in placodal cells and strongly in the migratory neuronal precursors (Fig. 3A,D), were not detected in *Eya1*^{−/−} distal VII, IX or X precursors (Fig. 3B,E and data not shown). Consistent with the observation of variable phenotype in the VIIth ganglion of *Six1*^{−/−} embryos detected with the *Neurog2* probe, two of six *Six1*^{−/−} embryos showed a few *Neurog1*-positive cells in the VIIth ganglion anlage bilaterally (Fig. 3C) and the other four embryos lacked *Neurog1* expression (data not shown). Similarly, *Neurog1* expression was markedly reduced in the IXth (Fig. 3F) and present at lower levels in the Xth precursors in all six *Six1*^{−/−} embryos (data not shown). In sections through E9.5 wild-type epibranchial placodes, we found that *Neurod* is also expressed in cells within the placodal ectoderm prior to delamination, as well as in delaminated precursors undergoing migration toward the condensing VIIth, IXth and Xth ganglia (Fig. 3G,J). These data differ slightly from previously reported expression only in migrating precursors in the mouse (Fode et al., 1998). Expression of *Neurod* in *Eya1*^{−/−} epibranchial precursors was absent (Fig. 3H,K), lacking in the *Six1*^{−/−} VIIth ganglion in four of six embryos (Fig. 3I) and reduced in IXth and Xth ganglia in all six embryos analyzed (Fig. 3L). Only a few *Neurod*-positive cells were observed in the VIIth precursors bilaterally in two of six *Six1*^{−/−} embryos (data not shown). Similarly, a few *Math3*- or *Nscl1*-positive cells were observed in the VIIth anlage in two of six *Six1*^{−/−} embryos bilaterally for both probes (data not shown and Fig. 3R), while their expression was largely reduced in the IXth and slightly reduced in the Xth anlage in all six *Six1*^{−/−} embryos (Fig. 3O,R). In *Eya1*^{−/−} embryos, a few *Math3*- and *Nscl1*-positve cells were also observed in *Eya1*^{−/−} Xth anlage unilaterally or bilaterally in all six embryos analyzed (Fig. 3N,Q). Together, the lack of expression of these markers further suggests that *Eya1* functions upstream of the *Neurog2*-regulatory pathway, and loss of Eya1 leads to the inactivation of the genetic program controlling sensory neuronal fate that normally expresses these bHLH genes.

Defective expression of *Phox2a* and *Phox2b* in *Eya1*^{−/−} and *Six1*^{−/−} cranial ganglia

During the development of the cranial sensory ganglia, the paired homeodomain protein Phox2a controls noradrenergic traits by blocking the transient expression of dopamine-β-hydroxylase (DBH), the terminal biosynthetic enzyme for norepinephrine (noradrenaline), and the expression of the related homeodomain protein Phox2b and the GDNF receptor subunit Ret (Morin et al., 1997; Pattyn et al., 1997). As *Phox2a* and *Neurog2* are activated independently, the neuronal subtype identity controlled by Phox2a is genetically independent from a subprogram for pan-neuronal gene expression controlled by Neurog2 (Fode et al., 1998). *Phox2a* is expressed in the epibranchial placodes and migrating precursors (Fig. 4A), while *Phox2b* is only expressed in the cells aggregating to form the ganglia (Fig. 4B) (Pattyn et al., 1997). In *Eya1*^{−/−} embryos, the expression of *Phox2a* and *Phox2b* was also abolished in the VIIth and IXth precursors (Fig. 4C,D), whereas weak *Phox2a* expression as well as very few *Phox2b*-expressing cells were observed in the Xth precursors (Fig. 4C,D). Section in situ hybridization at E9.0–10.0 further confirmed this observation (data not shown). In contrast, *Six1*^{−/−} embryos showed relatively normal *Phox2a* and *Phox2b* expression in the Xth, reduced in the IXth and absent (for *Phox2a*) or markedly reduced (for *Phox2b*) in the VIIth precursors in all four embryos analyzed (Fig. 4E,F), consistent with the observation of variable phenotype in *Six1*^{−/−} distal cranial ganglia (Figs 2, 3). While our observation of weak *Phox2a* expression in *Eya1*^{−/−} Xth precursors suggests that *Phox2* genes may be independent of *Eya1* in subsets of the Xth ganglion, lack of *Phox2*

expression in the VIIth and IXth and significant reduction in the Xth ganglia suggests that *Eya1* and *Six1* are required for the specification of sensory neuronal subtype precursors that normally express *Phox2* genes.

To further define the consequences of the early block in delamination of placodal precursors and test whether the cranial neural crest cells might migrate to populate the distal ganglia, we examined the development of the distal ganglia at later stages. Histological analysis at E11.5 to birth and marker staining with neurofilament at E11.5–13.5 revealed that *Eya1*$^{-/-}$ embryos completely lacked the epibranchial placode-derived distal VIIth and IXth cranial ganglia (Fig. 5). However, partial structure of the distal Xth ganglion was observed in *Eya1*$^{-/-}$ embryos (Fig. 5E). In *Six1*$^{-/-}$ embryos, while the VIIth ganglion was completely absent in all four embryos at each stage, the IXth ganglion was present but reduced in size and the Xth ganglion was relatively normal in all embryos (Fig. 5C,F,I,L). Taken together, these analyses further confirmed an early arrest of neurogenesis in the mutants and that in the absence of Eya1 or Six1, the cranial neural crest cells are unable to populate the distal ganglia, differing from *Neurog2* mutants (Fode et al., 1998).

Presence of proximal ganglia and rerouting of motor neurons of the facial nucleus through the trigeminal system in the mutants

As the distal ganglia in the mutants failed to recover at later stages, we further examined the development of the neural crest-derived proximal ganglia of the VIIth, IXth and Xth cranial nerves. The transcription factor Sox10 has been shown to be essential for the formation of sensory ganglia of the head and trunk, which are derived from neural crest cells, and it acts as a key regulator of peripheral glial development (Britsch et al., 2001). We therefore used *Sox10* as a probe to label the cranial sensory ganglia. The anlagen of the proximal VII, IX and X ganglia was brightly stained with *Sox10* and readily visible in E9.5–10.5 mutant and normal embryos (Fig. 6A–C), confirming the presence of some neural crest-derived proximal VII, IX and X ganglia in both mutants at these stages. This was further confirmed with neurofilament antibody staining (Fig. 6D–F and Fig. 5A–F). Interestingly, whole-mount *Sox10* and neurofilament staining revealed that the most posterior portion of the distal Xth ganglion was present in *Eya1*$^{-/-}$ embryos (arrowhead, Fig. 6B,E). Development of the Vth ganglion also appeared to be affected by the mutations as its size appeared to be somewhat reduced in *Eya1*$^{-/-}$ and *Six1*$^{-/-}$ embryos (Fig. 6B,C,E,F). Nerves originating from the Vth ganglion sometimes innervate the second branchial arches in both mutants (open arrowheads, Fig. 6B,C,F). This could be due to V projection error or to routing errors of caudal branchial motor fibers through the Vth ganglion.

To further confirm this observation and examine the consequence of the loss of the cranial VII and VIII sensory ganglia for the development of the associated cranial nerves, we performed retrograde as well as anterograde labeling of cranial nerve organization and their projection at E12.5 (data not shown) and E13.5. Application of lipophilic fluorescent dyes to the cranial nerves V (red) and VII/VIII (green) from the periphery resulted in labeling of V and VII motoneurons, V, VII and VIII afferents, and V and VII roots in normal embryos (Fig. 6G–I). In E13.5 *Eya1*$^{-/-}$ and *Six1*$^{-/-}$ mutant embryos, no VIIIth nerve projection and VII motoneurons and afferents were labeled after DiI application to the VII/VIII nerve injections from the periphery (Fig. 6H,N,I,O). However, VII motor neurons could be filled from the V nerve injections in both mutants (Fig. 6H,N,I,O). While a small projection of VII fibers out of the Vth ganglion was labeled in *Eya1*$^{-/-}$ embryos (Fig. 6N), some VII motor neurons reroute directly into the Vth ganglion inside the brainstem (arrow, Fig. 6O) or project outside the brain only to join the V nerve (arrow, Fig. 6I) in *Six1*$^{-/-}$ embryos. This observation suggests that our earlier data of abnormal fiber projections of the V system in the mutants (Fig. 6B,C,F) actually display the misrouting of VII branchial motoneurons.

Beyond the routing errors to and in peripheral nerves, we also observed altered trajectories of fibers in the brainstem. In wild-type mice, a sensory component of the V tract, the mesencephalicus V (MesV) component normally runs with other V fibers in the descending V tract (Fig. 6J). However, in both mutants, this tract runs in the area of the alar plate that normally receives the inner ear projection (Fig. 6H,I). In addition, expansion of the central projection of the V system was obvious in the mutants (Fig. 6K,L). An application of a long filter strip to all pre- and post-otic motoneurons in the basal plate, and an application of a different colored lipophilic tracer to the post-otic alar plate, labeled reliably the inner ear efferents and the VII nerve around the ear in wild-type animals (Fig. 6P). In *Eya1*$^{-/-}$ embryos, however, it only labeled a few IX/X sensory neurons (red), abducens (VI), V and trochlear (IV) nerves (all green, Fig. 6Q). In *Six1*$^{-/-}$ embryos, VII motoneurons exit separately but join the V fibers outside the brain (Fig. 6R,I). These data indicate that all inner ear innervation including inner ear efferents is missing and the VIIth nerve motoneurons, if present at all, exit with the Vth nerve in both mutants.

Six1 expression in the epibranchial placode is *Eya1* dependent

We have previously reported that murine *Eya1* is expressed in the cranial placodes including the epibranchial placodes at E9.5 (Xu et al., 1997a). However, the *Six1* expression in the epibranchial placodes during mouse development and the detailed relationship between the expression of these two genes in the generation of epibranchial placode-derived sensory neurons have not been studied. We therefore set out to establish how the expression of these genes related to the region and period of expression of *Neurog2*. *Eya1* expression was observed in all three epibranchial placodes as early as E8.5 (before turning of the embryos). In transverse sections of E8.5 to 10.5 embryos, *Eya1* expression was detected in the placodal cells, migrating precursors and developing ganglia (Fig. 7A,B and data not shown). However, no *Eya1* expression was observed in the V placodal cells at these stages (data not shown). X-gal staining of heterozygous *Six1*^{lacZ} embryos at E8.5 to 10.0, which recapitulated the *Six1* mRNA expression pattern (Xu et al., 2003; Zheng et al., 2003), revealed that *Six1* is strongly expressed in the distal VIIth and IXth placodal precursor cells and weakly in the Xth placodal precursors in E8.5 (before turning) embryos (data not shown). From E9.0 to 10.0, its expression is observed in placodal, migrating, and aggregating neuronal precursors in ganglion anlagen (Fig. 7C,D,H). Similar to *Eya1*, no *Six1* expression is observed in the V placodal cells (data not shown). Therefore, *Six1* appears to be expressed as early as *Eya1* in the distal epibranchial placodes, and both slightly precede *Neurog2* (Fode et al., 1998).

As *Eya1* acts upstream of *Six1* during otic placodal development (Zheng et al., 2003), we examined their expression in respective mutant embryos to test whether both genes also function in the same genetic pathway during epibranchial placodal development. Interestingly, *Eya1* expression was unaffected in *Six1*$^{-/-}$ epibranchial placodes at E9.0–10.0 (Fig. 7F,G), but *Six1* expression was undetectable in *Eya1*$^{-/-}$ epibranchial placodes at E9.5 (Fig. 7I), suggesting that the *Eya1-Six1* regulatory pathway also operates in the epibranchial placodal development.

Bmp7 expression in the pharyngeal endoderm is preserved in the mutants

Bmp7 in the pharyngeal endoderm has been shown to act as a signaling molecule for epibranchial placode induction and it can induce *Phox2a*-positive neurons directly from non-epibranchial placode head ectoderm (Begbie et al., 1999). In addition to the pharyngeal ectoderm, *Eya1* and *Six1* are expressed in the pharyngeal endoderm and neural crest mesenchyme (Xu et al., 2002). We therefore examined *Bmp7* expression in *Eya1*$^{-/-}$ and *Six1*$^{-/-}$ pharyngeal endoderm and found that its expression was unaffected (Fig. 7E,J and

data not shown). Thus, Eya1 and Six1 may function cell-autonomously in early development of epibranchial sensory neurons.

Increased cell death in the mutant epibranchial placodes

To look into the absence of neuronal precursor cells in $Eya1^{-/-}$ embryos, we carried out TUNEL labeling to determine whether the placodal ectodermal cells undergo abnormal apoptosis. More cell death was apparent in E10.0 $Eya1^{-/-}$ placodes (Fig. 8A–D). Apoptotic cells were also increased in the VIIth precursors but were relatively normal in the IXth and Xth precursors in all three $Six1^{-/-}$ embryos analyzed (data not shown). This analysis suggests that upon the failure to activate their normal developmental program, the progenitor cells undergo apoptosis in the mutant embryos.

Discussion

Neurons of cranial sensory ganglia with different embryonic origins have to develop appropriate ganglia, and send out processes both peripherally to the proper target regions and cells, and to their central target nuclei within the hindbrain (Cordes, 2001; Fritzsch, 2003; Maklad and Fritzsch, 2003b). Although it is known that the neurons of the proximal ganglia and VIII are specified by Neurog1, while the epibranchial neurons are determined by Neurog2 (Fode et al., 1998; Ma et al., 1998; Ma et al., 1999), the cellular and molecular mechanisms driving these processes are not well understood. Our results show that in the absence of Eya1 or Six1, the neuroblast precursors whose specification requires Neurog1 function were present. In contrast, the distal ganglia of the VIIth, IXth and Xth cranial nerves that require Neurog2 function for their normal development were absent in $Eya1^{-/-}$ and $Six1^{-/-}$ embryos. Furthermore, we show that disruption of the sensory ganglion formation leads to further patterning defects of branchial motoneurons in the cranial nerves. These analyses now define a specific role for both genes in cranial nerve patterning and diversification.

The role of Eya1 and Six1 during neurogenesis of the inner ear

The otic ectoderm is programmed for neurogenesis of the VIIIth ganglion from as early as a stage before the otic placode even becomes morphologically apparent. Recent studies have found that many genes are required for normal neurogenesis, but little is known of the cellular mechanisms involved in their development. In this study, we carefully assessed neurogenesis of the VIIIth ganglion in *Eya1* and *Six1* mutants, using *Neurog1* and *Neurod* as early molecular markers, and have now demonstrated that both *Eya1* and *Six1* genes are dispensable for the initiation of neurogenesis. However, our finding that lack of Eya1 or Six1 reduces the population of neuroblast precursors within the otic ectoderm indicates their requirement for maintenance of neurogenesis. Since *Neurog1* expression level is relatively normal in *Neurog1*-positive cells that are detected in the mutant otic ectoderm, but the number of *Neurog1*-positive cells was markedly reduced in the null mutant embryos (Fig. 1), one likely explanation for the reduction of neurogenesis within the otic ectoderm is that Eya1 and Six1 are required for proliferation of neuroblast progenitors. Consistent with this idea, pulse-chase BrdU incorporation studies revealed fewer BrdU-labeled cells in the ventral region within which the neuroblasts are normally specified in the mutant embryos from as early as E8.75 (Zheng et al., 2003). In addition, abnormal apoptosis occurred in the mutant otic ectoderm and might also contribute to the reduction of neuroblast progenitors, as detected by TUNEL assay (Xu et al., 1999; Zheng et al., 2003).

After specification, the neuroblast precursors normally migrate away from the ectoderm and aggregate to form the VIIIth ganglion. This epithelial-mesenchymal transition involves a number of changes in the delaminating precursors and their overt differentiation can be

induced and enhanced by extracellular matrix (ECM) (Hay, 1993). Our data also demonstrated that both Eya1 and Six1 are not required for neuroblast delamination (Fig. 1). As abnormal apoptosis, which probably reflects the death of *Eya1*- or *Six1*-dependent precursor cells, was observed in the mutant ganglion anlage that has not yet expressed *SCG10* (Fig. 2), they might regulate the progressive differentiation of the precursor cells. It should be noted that *Eya1* and *Six1* are also expressed in the periotic mesenchyme. However, it is unclear whether loss of their mesenchymal expression also contributes to the defect. Tissue-specific deletion of Eya1 or Six1 would be required to address the relative contribution of their expression in the mesenchyme to the development of the otic ganglion. Nonetheless, our results at earlier stages suggest that both Eya1 and Six1 regulate early neuronal differentiation and maintenance.

Conserved molecular mechanisms underlying epibranchial placodes

In addition to the otic placode, *Eya1* and *Six1* are coexpressed in other neurogenic placodes and cranial sensory ganglia (Xu et al., 1997a; Sahly et al., 1999; David et al., 2001). Studies in *Drosophila* eye imaginal disc indicate that *eya* is epistatic to *so* and both genes cross-regulate each other to maintain their expression (Pignoni et al., 1997). Our finding that *Six1* expression in the epibranchial placodes is *Eya1* dependent suggests evolutionary conservation of the *Drosophila Eya-Six* regulatory cassette in the epibranchial placodal development, similar to that observed in early otic development (Zheng et al., 2003). In contrast to the common ear phenotype in both mutants, the phenotype in the distal cranial ganglia appears less severe in *Six1* than in *Eya1* mutants. As we found that *Six1* is almost expressed as early as *Eya1*, one classic explanation for this finding is functional redundancy with another coexpressed molecule. The closely related family member *Six4* is also expressed in the cranial sensory ganglion from early stages and shows an identical pattern with *Six1* (Oliver et al., 1995; Esteve and Bovolenta, 1999; Kobayashi et al., 2000; Pandur and Moody, 2000; Ghanbari et al., 2001; Ozaki et al., 2001). Although the onset of *Six4* expression during mouse embryonic development has not been described, in the chick *Six4* transcripts were detected in the ectodermal placodes, including olfactory, optic, otic, and all epibranchial placodes as early as they acquire their identity (Esteve and Bovolenta, 1999). Thus, *Six1* and *Six4* may compensate for each other's role in cranial sensory ganglia. Such a compensatory mechanism has been noted between different bHLH genes *Neurog2* and *Neurog1*, *Mash1* and *Math3*, or *Mash1* and *Neurog2* in neurogenesis (Ma et al., 1999; Tomita et al., 2000; Nieto et al., 2001), and for the paralogous *Pax3* and *Pax7*, and *Pax1* and *Pax9* genes in other developmental systems (Borycki et al., 1999; Peters et al., 1999). This could explain why the *Six1* mutant phenotype appears to be variable and less severe than that in the *Eya1* mutants and why the *Six4* mutant mice do not display an embryonic phenotype (Ozaki et al., 2001).

Our data show that while a few neuronal precursors form in the VIIth and VIIIth ganglia in the mutants, no traces of sensory neurons are found at E13.5. In the absence of any viable sensory neurons, VII motoneurons project through the V ganglion system in both mutants. This is consistent with previous findings of rerouting of V motor fibers into the VII nerve in the absence of a V ganglion (Ma et al., 2000) and supports the hypothesis that sensory neurons may attract branchial motoneuron fibers (Fritzsch and Northcutt, 1993). Central expansion into vestibular nuclei by somatosensory fibers has been noticed before (Fritzsch, 1990). However, the massive expansion seen in *Six1* and *Eya1* mutant mice may be related to both central and peripheral effects of these genes. It is of interest to note that haploinsufficiency for the human *EYA1* or *SIX1* results in branchio-oto-renal (BOR) syndrome, an autosomal dominant developmental disorder characterized by branchial clefts, hearing loss, and renal anomalies (Abdelhak et al., 1997; Ruf et al., 2004). Minor anomalies, which occur in less than 20% of affected patients, including facial nerve paresis, lacrimal

duct aplasia and gustatory lacrimation, were also described (Smith and Schwartz, 1998) and these features reflect anomalies in the cranial nerve trajectories.

Eya1, Six1 and epibranchial placode-derived sensory neurons

Delamination of neuronal precursors is the first morphological sign of differentiation during cranial placode neurogenesis. Among the transcription factors involved in early sensory neurogenesis, Neurog2 appears to be required for delamination of neuronal precursors, and this process is blocked in *Neurog2* mutant epibranchial placodes (Fode et al., 1998). Although Phox2a is also expressed in the epibranchial placodes, it does not control the delamination of neuronal progenitors and their aggregation into the ganglion anlagen (Morin et al., 1997). Our studies show that the initial expression of both Eya1 and Six1 occur in the ectoderm of epibranchial placodes prior to delamination, and expression of *Neurog2* and *Phox2a* is lost in the mutant embryos (Figs 2, 3), suggesting that Eya1 and Six1 function is required before delamination occurs. Therefore, Eya1 probably acts in the initial selection of neuronal precursors within the epibranchial placodal ectoderm and in the absence of Eya1, the initial *Neurog2-* and *Phox2a*-expressing cells may not be specified. As *Eya1* is also expressed in the migratory precursors as well as in the forming ganglia, it may regulate migration as well as aggregation during neuronal precursor differentiation.

As the epibranchial placode cells that express Phox2a also express the highest levels of *Neurog2* transcripts, the same signal might be involved in the induction of both genes, coupling the generic and neuronal identity subprogram (Lo et al., 1999). However, the nature of the inducing signal is currently unclear. Our results indicate that Eya1 may induce *Neurog2* and *Phox2a*. When Neurog2 and Phox2a are activated, they will trigger neuronal differentiation in the placodal ectodermal cells. Failure to activate their normal differentiation programs will result in apoptosis of these placodal ectodermal cells (Fig. 8). Consistent with the idea that Eya1 acts genetically upstream of Neurog2 and Phox2a, the distal sensory ganglion formation appears to be more severely affected in $Eya1^{-/-}$ embryos than in $Neurog2^{-/-}$ (Fode et al., 1998) or $Phox2a^{-/-}$ embryos (Morin et al., 1997). Our data suggest the existence of differential mechanisms controlling epibranchial neuronal differentiation between different placodes. Some epibranchial neurons completely failed to develop but others, e.g. the Xth ganglion, were partially present in $Eya1^{-/-}$ embryos, or were mildly affected in $Six1^{-/-}$ embryos. The same ganglia were also differentially affected in *Neurog2* and *Phox2a* mutant mice (Fode et al., 1998). Our results show that the Xth neurons appear to be more severely affected in $Eya1^{-/-}$ embryos than in $Neurog2^{-/-}$ embryos as judged by marker analysis (Figs 4, 5), consistent with the idea that *Eya1* functions upstream of *Neurog2*. Thus, although it is possible that different placodes respond to regional-specific signals, our studies clearly show that Eya1 and Six1 are required for both generic and subtype-specific gene expression in the epibranchial placodes by regulating the expression of *Neurog2* and *Phox2a*.

It is noteworthy that *Eya* and *Six* genes are also co-expressed in myogenic cells and are involved in the molecular network controlling muscle development (Heanue et al., 1999; Fougerousse et al., 2002; Laclef et al., 2003). Similar to the nervous system, muscle differentiation is crucially dependent on four bHLH factors, Myf5, MyoD, Myogenin and Mrf4 (Weintraub et al., 1991). In contrast to their early role in neurogenesis, recent data from muscle have suggested that *Eya* and *Six* genes seem to be involved in later steps of myogenic differentiation but do not activate the expression of Myf5, which acts as a myogenic determination factor that activates other bHLH myogenic factors (Fougerousse et al., 2002; Delfini and Duprez, 2004). Thus, the *Eya-Six* regulatory hierarchy may operate through a similar molecular network in nerves and muscles but acts at distinct steps between sensory neuronal and muscle differentiation programs.

Acknowledgments

References

Abdelhak S, Kalatzis V, Heilig R, Compain S, Samson D, Vincent C, Weil D, Cruaud C, Sahly I, Leibovici M, et al. A human homologue of the Drosophila eyes absent gene underlies branchio-oto-renal (BOR) syndrome and identifies a novel gene family. Nat Genet. 1997; 15:157–164. [PubMed: 9020840]

Adam J, Myat A, Le Roux I, Eddison M, Henrique D, Ish-Horowicz D, Lewis J. Cell fate choices and the expression of Notch, Delta and Serrate homologues in the chick inner ear: parallels with Drosophila sense-organ development. Development. 1998; 125:4645–4654. [PubMed: 9806914]

Ayer-Le Lievre CS, Le Douarin NM. The early development of cranial sensory ganglia and the potentialities of their component cells studied in quail-chick chimeras. Dev Biol. 1982; 94:291–310. [PubMed: 7152108]

Begbie J, Brunet JF, Rubenstein JL, Graham A. Induction of the epibranchial placodes. Development. 1999; 126:895–902. [PubMed: 9927591]

Bonini NM, Leiserson WM, Benzer S. The eyes absent gene: genetic control of cell survival and differentiation in the developing Drosophila eye. Cell. 1993; 72:379–395. [PubMed: 8431945]

Borsani G, DeGrandi A, Ballabio A, Bulfone A, Bernard L, Banfi S, Gattuso C, Mariani M, Dixon M, Donnai D, et al. *EYA4*, a novel vertebrate gene related to *Drosophila eyes absent*. Hum Mol Genet. 1999; 8:11–23. [PubMed: 9887327]

Borycki AG, Li J, Jin F, Emerson CP, Epstein JA. Pax3 functions in cell survival and in pax7 regulation. Development. 1999; 126:1665–1674. [PubMed: 10079229]

Britsch S, Goerich DE, Riethmacher D, Peirano RI, Rossner M, Nave KA, Birchmeier C, Wegner M. The transcription factor Sox10 is a key regulator of peripheral glial development. Genes Dev. 2001; 15:66–78. [PubMed: 11156606]

Buller C, Xu X, Marquis V, Schwanke R, Xu PX. Molecular effects of Eya1 domain mutations causing organ defects in BOR syndrome. Hum Mol Genet. 2001; 10:2775–2781. [PubMed: 11734542]

Chen R, Amoui M, Zhang Z, Mardon G. Dachshund and eyes absent proteins form a complex and function synergistically to induce ectopic eye development in *Drosophila*. Cell. 1997; 91:893–903. [PubMed: 9428513]

Cordes SP. Molecular genetics of cranial nerve development in mouse. Nat Rev Neurosci. 2001; 2:611–623. [PubMed: 11533729]

D'Amico-Martel A, Noden DM. Contributions of placodal and neural crest cells to avian cranial peripheral ganglia. Am J Anat. 1983; 166:445–468. [PubMed: 6858941]

David R, Ahrens K, Wedlich D, Schlosser G. Xenopus Eya1 demarcates all neurogenic placodes as well as migrating hypaxial muscle precursors. Mech Dev. 2001; 103:189–192. [PubMed: 11335132]

Delfini MC, Duprez D. Ectopic Myf5 or MyoD prevents the neuronal differentiation program in addition to inducing skeletal muscle differentiation, in the chick neural tube. Development. 2004; 131:713–723. [PubMed: 14724123]

Esteve P, Bovolenta P. cSix4, a member of the six gene family of transcription factors, is expressed during placode and somite development. Mech Dev. 1999; 85:161–165. [PubMed: 10415356]

Farinas I, Jones KR, Tessarollo L, Vigers AJ, Huang E, Kirstein M, de Caprona DC, Coppola V, Backus C, Reichardt LF, et al. Spatial shaping of cochlear innervation by temporally regulated neurotrophin expression. J Neurosci. 2001; 15:6170–6180. [PubMed: 11487640]

Fode C, Gradwohl G, Morin X, Dierich A, LeMeur M, Goridis C, Guillemot F. The bHLH protein NEUROGENIN 2 is a determination factor for epibranchial placode derived sensory neurons. Neuron. 1998; 20:483–494. [PubMed: 9539123]

Fougerousse F, Durand M, Lopez S, Suel L, Demignon J, Thornton C, Ozaki H, Kawakami K, Barbet P, Beckmann JS, Maire P. Six and Eya expression during human somitogenesis and MyoD gene family activation. J Muscle Res Cell Motil. 2002; 23:255–264. [PubMed: 12500905]

Fritzsch B. Experimental reorganization in the alar plate of the clawed toad, Xenopus laevis. I Quantitative and qualitative effects of embryonic otocyst extirpation. Brain Res Dev Brain Res. 1990; 51:113–122.

Fritzsch B. Development of inner ear afferent connections: forming primary neurons and connecting them to the developing sensory epithelia. Brain Res Bull. 2003; 60:423–433. [PubMed: 12787865]

Fritzsch B, Northcutt RG. Cranial and spinal nerve organization in amphioxus and lampreys: evidence for an ancestral craniate pattern. Acta Anat. 1993; 148:96–109. [PubMed: 8109201]

Ghanbari H, Seo HC, Fjose A, Brandli AW. Molecular cloning and embryonic expression of Xenopus *Six* homeobox genes. Mech Dev. 2001; 101:271–277. [PubMed: 11231090]

Hay ED. Extracellular matrix alters epithelial differentiation. Curr Opin Cell Biol. 1993; 5:1029–1035. [PubMed: 8129940]

Heanue TA, Reshef R, Davis RJ, Mardon G, Oliver G, Tomarev S, Lassar AB, Tabin CJ. Synergistic regulation of vertebrate muscle development by Dach2, Eya2, and Six1, homologs of genes required for Drosophila eye formation. Genes Dev. 1999; 13:3231–3243. [PubMed: 10617572]

Kim WY, Fritzsch B, Serls A, Bakel LA, Huang EJ, Reichardt LF, Barth DS, Lee JE. *NeuroD*-null mice are deaf due to a severe loss of the inner ear sensory neurons during development. Development. 2001; 128:417–426. [PubMed: 11152640]

Kobayashi M, Osanai H, Kawakami K, Yamamoto M. Expression of three zebrafish *Six4* genes in the cranial sensory placodes and the developing somites. Mech Dev. 2000; 98:151–155. [PubMed: 11044620]

Laclef C, Hamard G, Demignon J, Souil E, Houbron C, Maire P. Altered myogenesis in Six1-deficient mice. Development. 2003; 130:2239–2252. [PubMed: 12668636]

Le Douarin NM. Ontogeny of the peripheral nervous system from the neural crest and the placodes. A developmental model studied on the basis of the quail-chick chimaera system. Harvey Lect. 1984; 80:137–186. [PubMed: 6400655]

Lee JE, Hollenberg SM, Snider L, Turner DL, Lipnick N, Weintraub H. Conversion of Xenopus ectoderm into neurons by NeuroD, a basic helix-loop-helix protein. Science. 1995; 268:836–844. [PubMed: 7754368]

Lo L, Morin X, Brunet JF, Anderson DJ. Specification of neurotransmitter identity by Phox2 proteins in neural crest stem cells. Neuron. 1999; 22:693–705. [PubMed: 10230790]

Ma Q, Anderson DJ, Fritzsch B. Neurogenin 1 null mutant ears develop fewer, morphologically normal hair cells in smaller sensory epithelia devoid of innervation. J Assoc Res Otolaryngol. 2000; 1:129–143. [PubMed: 11545141]

Ma Q, Chen Z, del Barco Barrantes I, de la Pompa JL, Anderson DJ. Neurogenin1 is essential for the determination of neuronal precursors for proximal cranial sensory ganglia. Neuron. 1998; 20:469–482. [PubMed: 9539122]

Ma Q, Fode C, Guillemot F, Anderson DJ. Neurogenin1 and neurogenin2 control two distinct waves of neurogenesis in developing dorsal root ganglia. Genes Dev. 1999; 13:1717–1728. [PubMed: 10398684]

Maklad A, Fritzsch B. Partial segregation of posterior crista and saccular fibers to the nodulus and uvula of the cerebellum in mice, and its development. Brain Res Dev Brain Res. 2003a; 140:223–236.

Maklad A, Fritzsch B. Development of vestibular afferent projections into the hindbrain and their central targets. Brain Res Bull. 2003b; 60:497–510. [PubMed: 12787869]

Mark M, Lufkin T, Vonesch JL, Ruberte E, Olivo JC, Dolle P, Gorry P, Lumsden A, Chambon P. Two rhombomeres are altered in Hoxa1 mutant mice. Development. 1993; 119:319–338. [PubMed: 8287791]

Moody SA, Heaton MB. Developmental relationships between trigeminal ganglia and trigeminal motoneurons in chick embryos. I Ganglion development is necessary for motoneuron migration. J Comp Neurol. 1983; 213:327–343. [PubMed: 6601116]

Morin X, Cremer H, Hirsch MR, Kapur RP, Goridis C, Brunet JF. Defects in sensory and autonomic ganglia and absence of locus coeruleus in mice deficient for the homeobox gene *Phox2a*. Neuron. 1997; 18:411–423. [PubMed: 9115735]

Nieto M, Schuurmans C, Britz O, Guillemot F. Neural bHLH genes control the neuronal versus glial fate decision in cortical progenitors. Neuron. 2001; 29:401–413. [PubMed: 11239431]

Oliver G, Wehr R, Jenkins NA, Copeland NG, Cheyette BN, Hartenstein V, Zipursky SL, Gruss P. Homeobox genes and connective tissue patterning. Development. 1995; 121:693–705. [PubMed: 7720577]

Ozaki H, Watanabe Y, Takahashi K, Kitamura K, Tanaka A, Urase K, Momoi T, Sudo K, Sakagami J, Asano M, Iwakura Y, Kawakami K. Six4, a putative myogenin gene regulator, is not essential for mouse embryonal development. Mol Cell Biol. 2001; 21:3343–3350. [PubMed: 11313460]

Pandur PD, Moody SA. Xenopus *Six1* gene is expressed in neurogenic cranial placodes and maintained in the differentiating lateral lines. Mech Dev. 2000; 96:253–257. [PubMed: 10960794]

Pattyn A, Morin X, Cremer H, Goridis C, Brunet JF. Expression and interactions of the two closely related homeobox genes Phox2a and Phox2b during neurogenesis. Development. 1997; 124:4065–4075. [PubMed: 9374403]

Pattyn A, Morin X, Cremer H, Goridis C, Brunet JF. The homeobox gene Phox2b is essential for the development of autonomic neural crest derivatives. Nature. 1999; 399:366–370. [PubMed: 10360575]

Pattyn A, Hirsch M, Goridis C, Brunet JF. Control of hindbrain motor neuron differentiation by the homeobox gene Phox2b. Development. 2000; 127:1349–1358. [PubMed: 10704382]

Peters H, Wilm B, Sakai N, Imai K, Maas R, Balling R. Pax1 and Pax9 synergistically regulate vertebral column development. Development. 1999; 126:5399–5408. [PubMed: 10556064]

Pignoni F, Hu B, Zavitz KH, Xiao J, Garrity PA, Zipursky SL. The eye specification proteins So and Eya form a complex and regulate multiple steps in Drosophila eye development. Cell. 1997; 91:881–891. [PubMed: 9428512]

Ruf RG, Xu PX, Silvius D, Otto EA, Beekmann F, Muerb UT, Kumar S, Neuhaus TJ, Kemper MJ, Berkman J, et al. *SIX1* mutations cause branchio-oto-renal syndrome by disruption of EYA1-SIX1-DNA complexes. Proc Natl Acad Sci USA. 2004; 101:8090–8095. [PubMed: 15141091]

Sahly I, Andermann P, Petit C. The zebrafish *eya1* gene and its expression pattern during embryogenesis. Dev Genes Evol. 1999; 209:399–410. [PubMed: 10370123]

Schlosser G, Ahrens K. Molecular anatomy of placode development in Xenopus laevis. Dev Biol. 2004; 271:439–466. [PubMed: 15223346]

Smith RJ, Schwartz C. Branchio-oto-renal syndrome. J Commun Disord. 1998; 31:411–420. [PubMed: 9777487]

Tomita K, Moriyoshi K, Nakanishi S, Guillemot F, Kageyama R. Mammalian achaete-scute and atonal homologs regulate neuronal versus glial fate determination in the central nervous system. EMBO J. 2000; 19:5460–5472. [PubMed: 11032813]

Weintraub H, Davis R, Tapscott S, Thayer M, Krause M, Benezra R, Blackwell TK, Turner D, Rupp R, Hollenberg S, et al. The myoD gene family: nodal point during specification of the muscle cell lineage. Science. 1991; 251:761–766. [PubMed: 1846704]

Xu PX, Adams J, Peters H, Brown MC, Heaney S, Maas R. Eya1-deficient mice lack ears and kidneys and show abnormal apoptosis of organ primordia. Nat Genet. 1999; 23:113–117. [PubMed: 10471511]

Xu P-X, Cheng J, Epstein JA, Maas RL. Mouse Eya genes are expressed during limb tendon development and encode a transcriptional activation function. Proc Natl Acad Sci USA. 1997b; 94:11974–11979. [PubMed: 9342347]

Xu PX, Woo I, Her H, Beier DR, Maas RL. Mouse Eya homologues of the Drosophila eyes absent gene require Pax6 for expression in lens and nasal placode. Development. 1997a; 124:219–231. [PubMed: 9006082]

Xu PX, Zheng WM, Laclef C, Maire P, Maas RL, Peters H, Xu X. Eya1 is required for the morphogenesis of mammalian thymus, parathyroid and thyroid. Development. 2002; 129:3033–3044. [PubMed: 12070080]

Xu PX, Zheng W, Huang L, Maire P, Laclef C, Silvius D. Six1 is required for the early organogenesis of mammalian kidney. Development. 2003; 130:3085–3094. [PubMed: 12783782]

Zheng W, Huang L, Wei ZB, Silvius D, Tang B, Xu PX. The role of Six1 in mammalian auditory system development. Development. 2003; 130:3989–4000. [PubMed: 12874121]

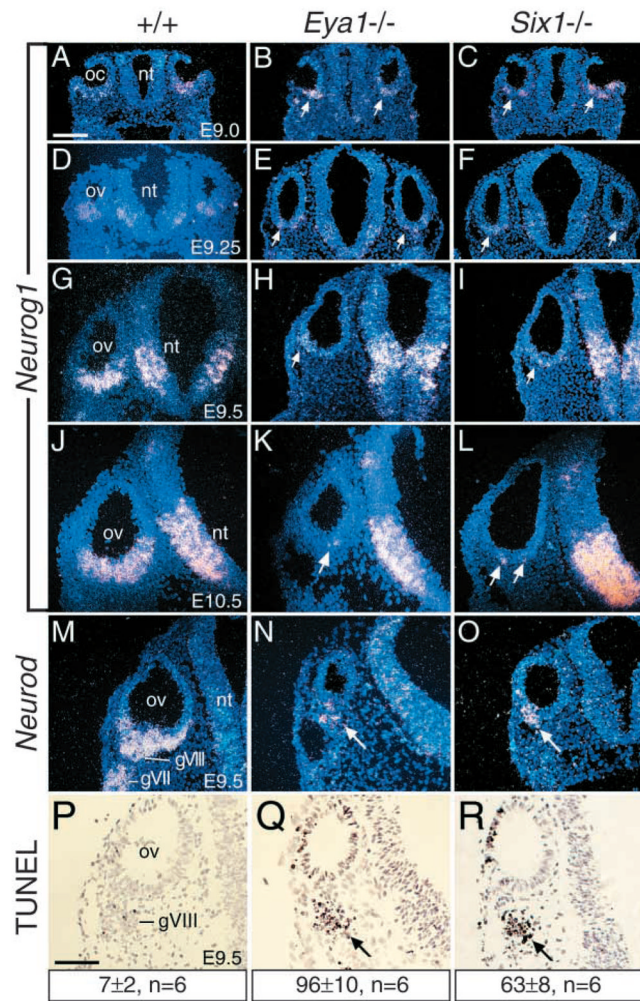**Fig. 1.**
Eya1 and Six1 are required for the maintenance of normal neurogenesis during inner ear morphogenesis. Section in situ hybridization on transverse sections through the otic region. (A–C) *Neurog1* is expressed in the ventral otic cup (oc) of E9.0 wild-type embryos (A), and its expression in $Eya1^{-/-}$ (B), and $Six1^{-/-}$ (C) embryos is indistinguishable from wild-type embryos. (D–L) *Neurog1* expression became stronger from E9.25 to 10.5 after the vesicle (ov) is closed up (D,G,J); however, its expression is markedly reduced in $Eya1^{-/-}$ (arrows in E,H) or $Six1^{-/-}$ (arrows in F,I) from E9.25, and by E10.5 only a few *Neurog1*-positive cells were seen in the $Eya1^{-/-}$ (arrow in H) or $Six1^{-/-}$ (arrows in L) otic vesicle. Note that *Neurog1* expression in the hindbrain neural tube (nt) is relatively normal in $Eya1^{-/-}$ or $Six1^{-/-}$ embryos compared to wild-type embryos. (M–O) *Neurod* is expressed in the differentiating neuroblast precursors within the otic vesicle (ov) and the cells migrating to form the VIIIth ganglion (gVIII) as well as within the VIIth ganglion (gVII) from E9.5 (M) in wild-type embryos. In $Eya1^{-/-}$ (N) or $Six1^{-/-}$ (O) embryos, *Neurod* expression in the cells within the otic vesicle and the cells migrating away from the otic vesicle was observed (arrow in N,O). (P–R) Transverse sections through E9.5 wild-type (P), $Eya1^{-/-}$ (Q) and $Six1^{-/-}$ (R) embryos labeled with the TUNEL method for detection of apoptotic cells. TUNEL-positive cells from 6 developing VIIIth ganglia (three embryos) for each genotype were counted using an image analysis system, and the number provided represents an

average number per ganglion for each genotype. Apoptosis was markedly induced in the mutants (arrow). Scale bar: 100 μm.
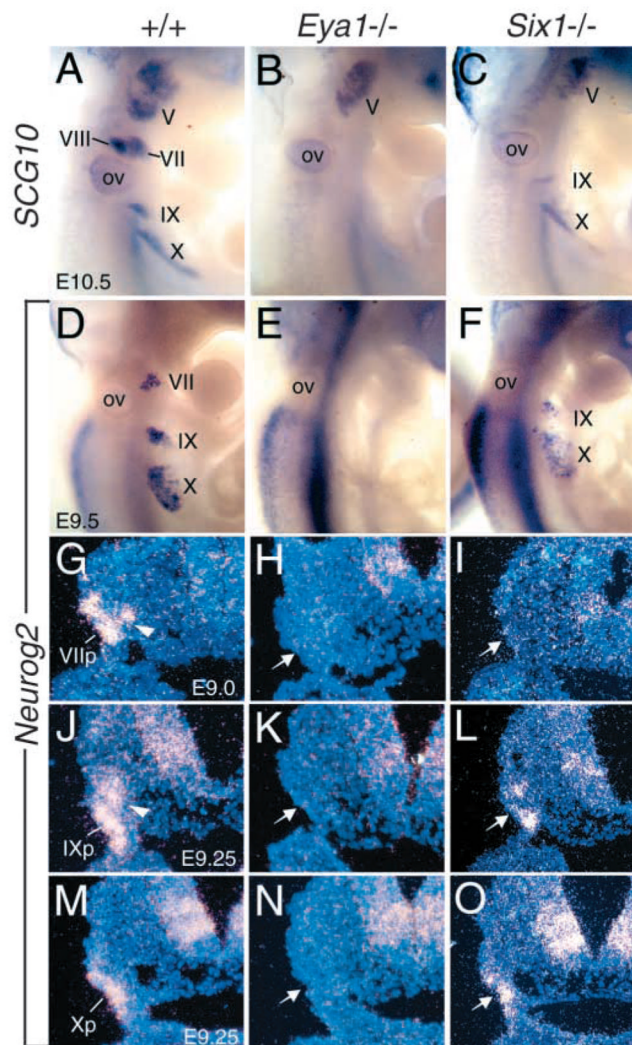
Fig. 2.
Deletion of distal cranial sensory ganglia in *Eya1*$^{-/-}$ and *Six1*$^{-/-}$ embryos. (A–C) Whole-mount hybridization with an *SCG10* riboprobe of wild-type (A), *Eya1*$^{-/-}$ (B), and *Six1*$^{-/-}$ (C) embryos at E10.5. A lack of neuronal differentiation of VIIIth and distal VIIth, IXth and Xth precursors is observed in *Eya1*$^{-/-}$ embryos. In *Six1*$^{-/-}$ embryos, *SCG10* staining was also missing in the regions of VIIIth and distal VIIth ganglia and slightly reduced in the regions of distal IXth and Xth ganglia. (D–F) E9.5 embryos hybridized with an *Neurog2* riboprobe. *Neurog2* expression in distal VII, IX and X placodes is readily visible in wild-type embryos, but its expression is completely lost in these structures in *Eya1*$^{-/-}$ embryos. In *Six1*$^{-/-}$ embryos, *Neurog2* expression is undetectable in the VIIth placode and markedly reduced in the IXth and reduced in Xth placode. (G–O) Section in situ hybridization with the *Neurog2* riboprobe of wild-type (G,J,M), *Eya1*$^{-/-}$ H,K,N) and *Six1*$^{-/-}$ (I,L,O) embryos at E8.5 to 9.25. Strong *Neurog2* expression was observed in the distal VIIth placode (VIIp), and some migratory precursors (arrowhead) at E8.5–9.0 and in the distal IXth placode (IXp), and migratory precursors (arrowhead) at E8.75–9.25 and the Xth placode (Xp) at E9.0–9.25 in wild-type embryos, whereas its expression is completely absent in these structures of *Eya1*$^{-/-}$ at these stages (arrow, H,K,N). In *Six1*$^{-/-}$ embryos, its expression was reduced to

background level in the VIIth precursors (arrow, I), also slightly reduced in the IXth (arrow, L) and relatively normal in the Xth precursors (arrow, O).
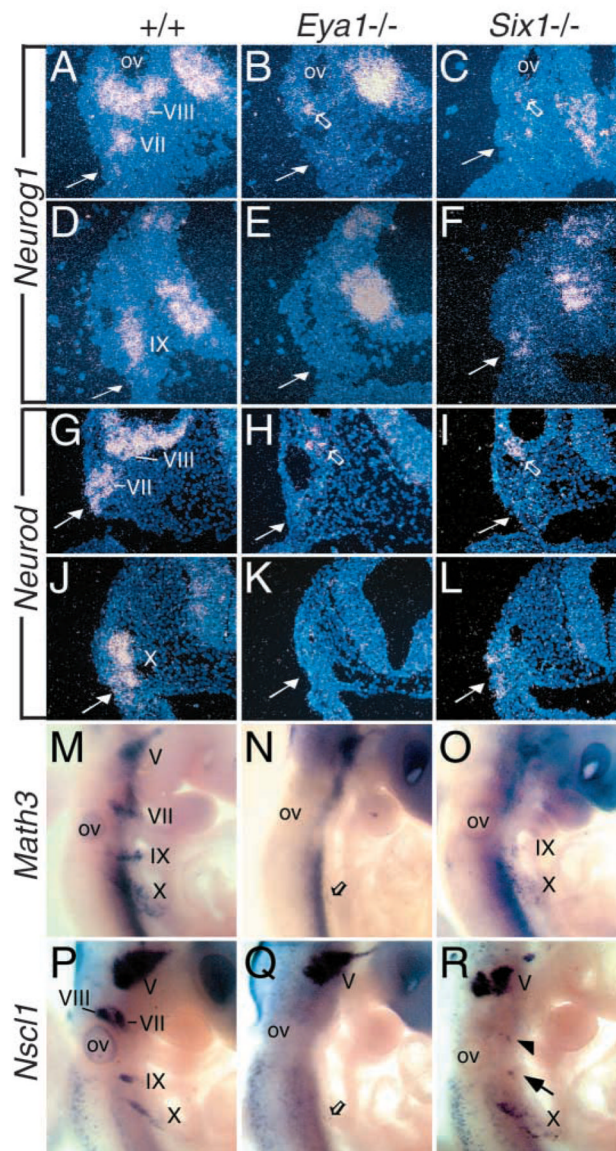
Fig. 3.
Alteration of *Neurog1*, *Neurod*, *Math3* and *Nscl1* expression in *Eya1*$^{-/-}$ and *Six1*$^{-/-}$ epibranchial neuronal precursors. (A–F) Transverse section hybridization showing *Neurog1* expression in the otic vesicle (ov) and in the VIIIth ganglion region and epibranchial (VII, IX) neuronal precursors in wild-type embryos (A,D), no expression in *Eya1*$^{-/-}$ epibranchial neuronal precursors (arrow in B,E) and reduced expression in *Six1*$^{-/-}$ epibranchial neurons (arrow in C,F). Note that *Neurog1* expression was observed in the VIIIth precursors (open arrow in B,C). (G–L) Transverse section hybridization showing *Neurod* expression in the VIIIth and epibranchial neuronal precursors in wild-type embryos (G,J), no expression in epibranchial precursors in *Eya1*$^{-/-}$ embryos (arrow in H,K) and no expression (arrow in I) or reduced expression in *Six1*$^{-/-}$ epibranchial neurons (arrow in L). Note that *Neurod* expression was detected in the VIIIth neuroblast precursors (open arrow in H,I). (M–O) Whole-mount hybridization showing *Math3* expression in epibranchial neurons in wild-type embryos (M), only a few *Math3*-positive cells in *Eya1*$^{-/-}$ Xth neurons (open arrow in N), and reduced expression in *Six1*$^{-/-}$ IXth and Xth neurons (O). (P–R) Whole-mount

hybridization showing *Nscl1* expression in cranial sensory ganglia in wild-type embryos (P). In *Eya1*$^{-/-}$ embryos, while *Nscl1* expression appeared relatively normal in the Vth ganglion, it expression is absent in VIIIth, VIIth and IXth ganglia and very few *Nscl1*-positive cells were detected in *Eya1*$^{-/-}$ Xth neurons (open arrow in Q). (R) *Nscl1* expression is also absent in *Six1*$^{-/-}$ VIIIth ganglion and markedly reduced in *Six1*$^{-/-}$ VIIth (arrowhead) and IXth (arrow) ganglia.
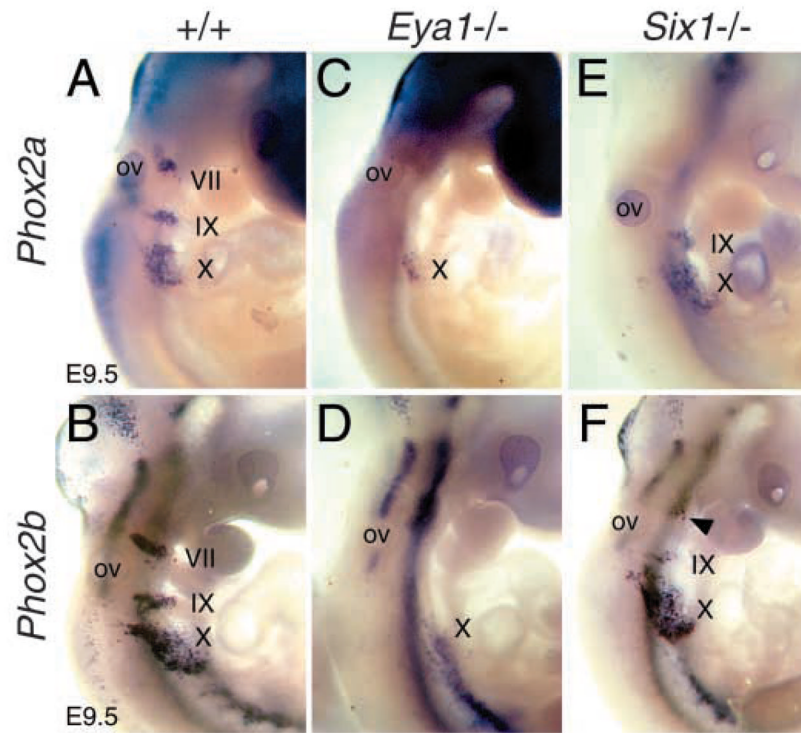
Fig. 4.
Alteration of *Phox2a* and *Phox2b* expression in *Eya1*$^{-/-}$ and *Six1*$^{-/-}$ epibranchial neuronal precursors. Whole-mount hybridization showing *Phox2a* (A) and *Phox2b* (B) expression in the epibranchial neurons in wild-type embryos. (C,D) In *Eya1*$^{-/-}$ embryos, weak *Phox2a* and *Phox2b* expression was only observed in the Xth neurons. (E,F) In *Six1*$^{-/-}$ embryos, their expression was absent (E) or markedly reduced in the VIIth (arrowhead in F), markedly reduced in the IXth, and relatively normal in the Xth neurons.
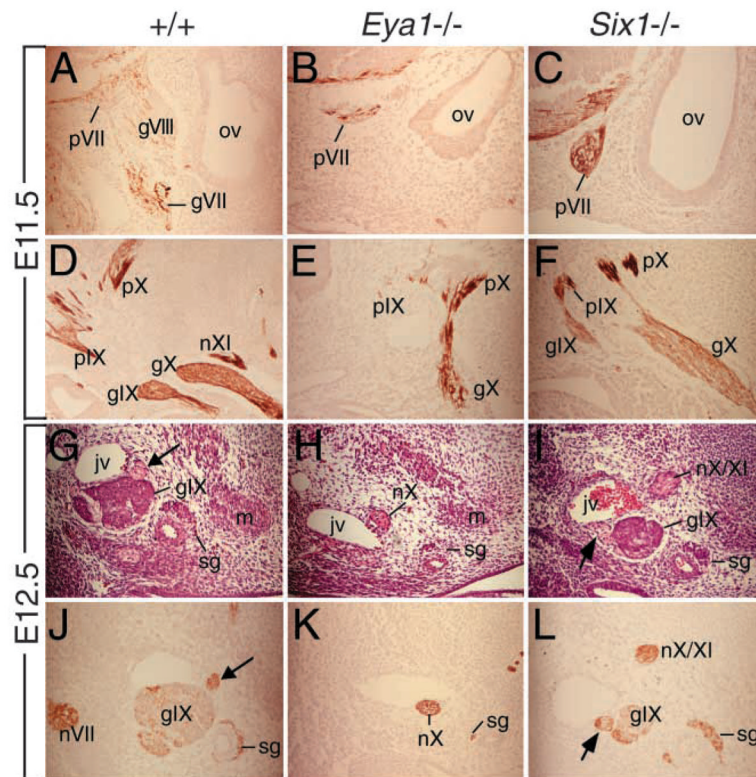
Fig. 5.

Malformation of cranial sensory ganglia in *Eya1*⁻/⁻ or *Six1*⁻/⁻ embryos at later stages. (A–F) Neurofilament antibody staining of sagittal sections of E11.5 wild-type (A,D), *Eya1*⁻/⁻ (B,E) and *Six1*⁻/⁻ (C,F) heads. Neurofilament antibody labeled the proximal VIIth ganglion (pVII), which is normally fused with the VIIIth ganglion (gVIII), the proximal IXth (pIX) and Xth (pX) and the distal VIIth (gVII), IXth (gIX) and Xth (gX) ganglia in wild-type embryos (A,D). In *Eya1*⁻/⁻ embryos, all proximal ganglia and partial structures of the distal Xth ganglion are present, but the VIIIth and the distal VIIth and IXth ganglia are missing (B,E). (C,F) In all three *Six1*⁻/⁻ embryos, while the proximal ganglia are present, the VIIIth and distal VIIth (gVII) ganglia are missing but the distal IXth and Xth ganglia are also present. For A–F, anterior is to the left and dorsal is up. (G–I) Hematoxylin and Eosin and (J–L) neurofilament antibody staining of transverse sections of E12.5 wild-type (G,J), *Eya1*⁻/⁻ (H,K) and *Six1*⁻/⁻ (I,L) heads. (G,J) The IXth ganglion (gIX) and the nerve fibers near the IXth ganglion that strongly stained with both Eosin and the neurofilament antibody are present in wild-type embryos (arrow). The neurofilament antibody also strongly labeled other nerve fibers in that region, including the VIIth nerve fibers (nVII, J). (G,K) The IXth ganglion is missing in *Eya1*⁻/⁻ embryos. However, some nerve fibers that strongly stained with both Eosin and the neurofilament antibody are present in the mutant and this structure is likely to represent the Xth nerve fibers, which are present at E11.5 (E). (I,L) The IXth ganglion is present in *Six1*⁻/⁻ embryos with slightly smaller size and the neurofilament antibody also labeled nearby nerve fibers (arrow and nX/XI). For G–L, dorsal is up and lateral is to the left. jv, internal jugular vein; m, prevertebral premuscle mass; sg, sympathetic ganglion component.
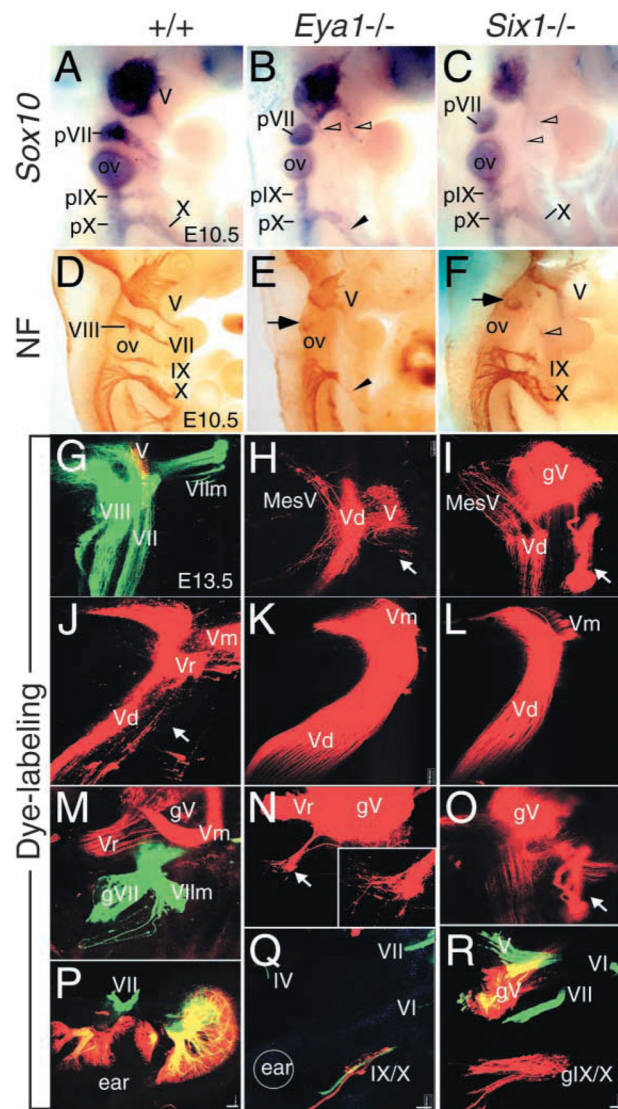
Fig. 6.
Eya1 and Six1 regulate the patterning of cranial sensory nerves and their associated ganglia. (A–C) E10.5 whole-mount embryos hybridized with a *Sox10* riboprobe. The proximal VIIth (pVII), IXth (pIX) and Xth (pX) ganglia are present in *Eya1*$^{-/-}$(B) or *Six1*$^{-/-}$ (C) embryos. Truncated distal Xth ganglion (X) is present in *Eya1*$^{-/-}$ embryos (arrowhead, B). (D–F) E10.5 whole-mount embryos immunostained with an antibody against Neurofilament (NF). The VIIIth and distal VIIth, IXth and Xth ganglia are apparent in wild type embryos (D). However, the VIIIth and the distal VIIth ganglia are missing in *Eya1*$^{-/-}$ (E) and *Six1*$^{-/-}$ (F) embryos. While the distal IXth is completely absent but the distal Xth ganglion is truncated in *Eya1*$^{-/-}$ (arrowhead, E), both are present in *Six1*$^{-/-}$ embryos (F). Arrow points to the proximal VIIth ganglion in the mutants (E,F). Nerves originating from the Vth ganglion sometime innervate the second branchial arches in both mutants (open arrowheads). (G–R) Whole-mount images of E13.5 wild-type (G,J,M,P), *Eya1*$^{-/-}$ (H,K,N,Q) and *Six1*$^{-/-}$ (I,L,O,R) embryos show the development of cranial nerves using lipophilic dyes to trace the fibers from the nerves into the brain (G–O) and from the brain to the periphery (P–R). (G) An image shows the VIII projection (left two layers; vestibular and cochlear projection), the V/VII projection (green), the VII motor root (VIIm, green) and partial V projection (red) in

normal animals. (H) There is no VIII nerve projection in any E13.5 *Eya1*−/− or (I) *Six1*−/− animals after applications to the hyoid (VII nerve) arch. However, the VII motoneurons were filled from the V nerve in both mutants (arrow). In addition, a V sensory component (MesV) projects not into the descending V (Vd) tract but rather into the area that receives the inner ear projection in normal animals. (J) A whole-mount image shows the V descending tract (Vd), V root (Vr) and motoneurons (Vm) in E13.5 normal animals. (K,L) Images show obvious expansion of the V projection in *Eya1*−/− (K) and *Six1*−/− (L) embryos. (M) V (red) and VII (green) ganglia and roots are shown as they approach the brain. (N) There is small projection of VII fibers out of the V ganglion in *Eya1*−/− animals (arrow). (O) In *Six1*−/− embryos, some VII motoneurons reroute directly into the V ganglion (gV) (arrow) or project outside the brain only to join the V nerve (compare images of I and O, which are taken form a lateral and a medial perspective of the same brain). (P) A motoneuron injection (green) and a sensory alar plate injection (red) caudal to the ear labels the VIII and VII nerves around the ear. (Q) In *Eya1*−/− embryos, only a few sensory neurons of the IX/X ganglia (red), abducens (VI), V and trochlear (IV) nerves (all green) are labeled. Circle indicates the approximate position of the ear. (R) In this *Six1*−/− animal, the VII motoneurons exit separately from V but join the V fibers outside the brain. Note the more profound reduction in IX/X ganglion size in *Eya1* mutants (Q,R). Anterior is up and dorsal is to the left in all images. Scale bar: 100 μm.
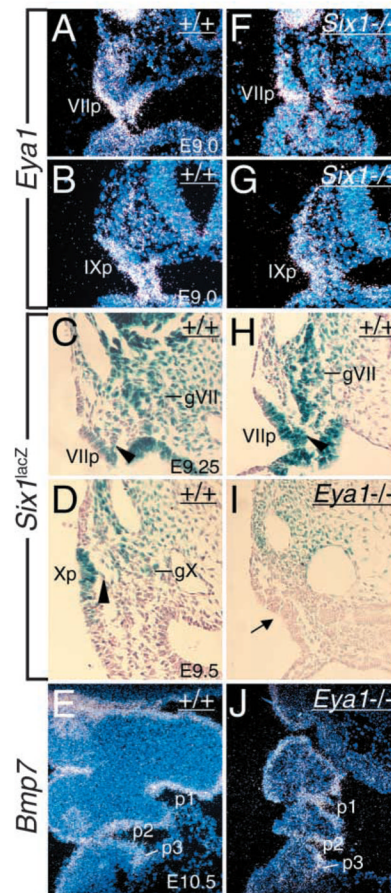
Fig. 7.
Eya1 controls *Six1* expression in epibranchial placodes. (A,B,F,G) Transverse sections showing *Eya1* expression in distal VIIth placode (VIIp, A) at E9.0 and distal IXth placode (pIX, B) at E9.0 and its expression in these structures was preserved in *Six1*$^{-/-}$ embryos (F,G). (C,D,H,I) Transverse sections showing *Six1*^{lacZ} expression in distal VIIth, IXth and Xth placodal, migratory (arrowhead) and aggregating neuronal precursors in the ganglion anlagen (gVII, gIX, gX) at E9.25–9.5 in *Six1*$^{lacZ/+}$ heterozygous embryos (C,D,H) and its expression was undetectable in *Eya1*$^{-/-}$ epibranchial neuronal precursors (I). (E,J) *Bmp7* expression in the pharyngeal pouches (p1–p3, E) at E10.5 was unaffected in *Eya1*$^{-/-}$ embryos (J).
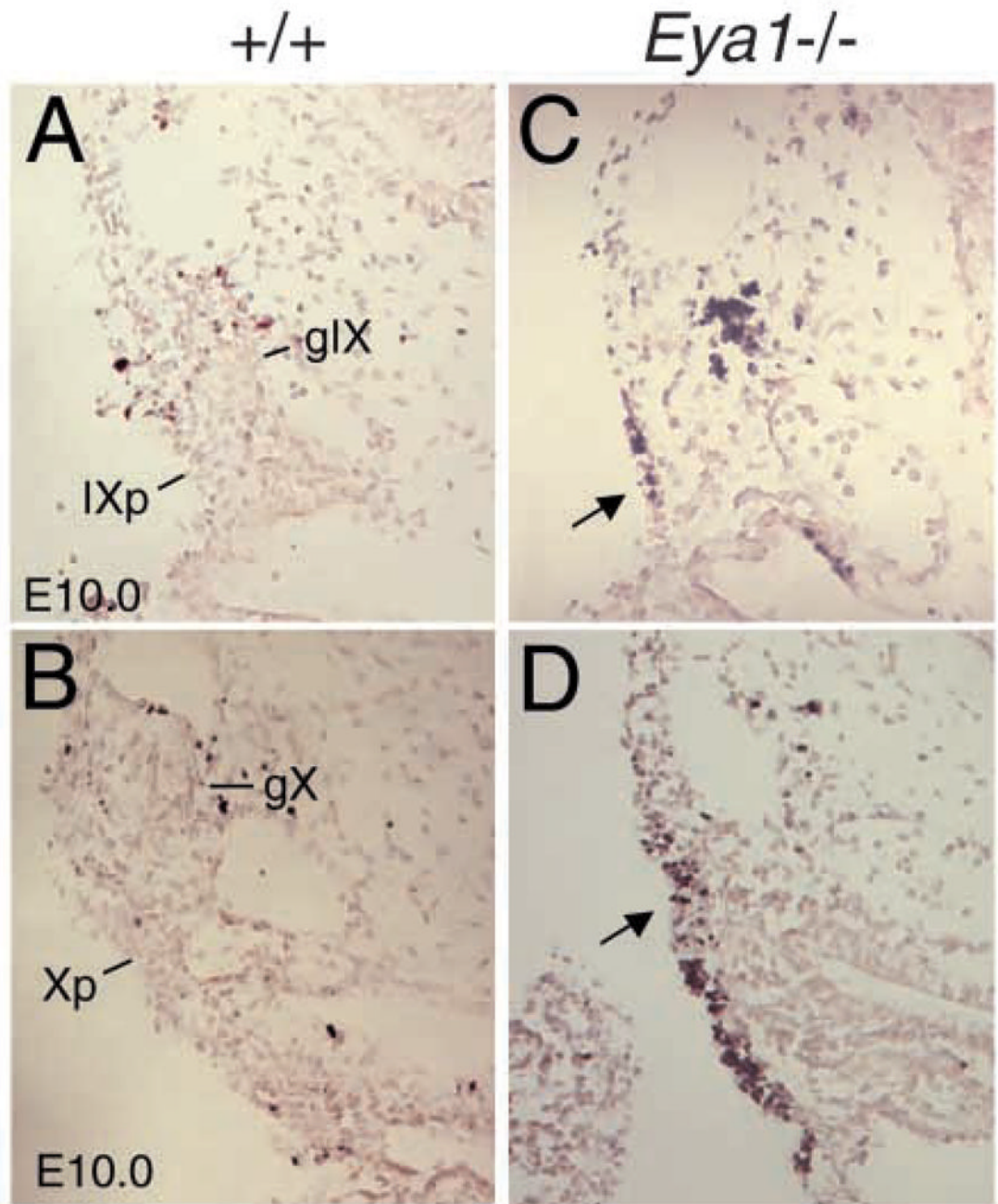
Fig. 8.
Eya1$^{-/-}$ placodal progenitor cells undergo abnormal apoptosis. Transverse sections labeled with the TUNEL method for detection of apoptotic cells showing a few apoptotic cells in the wild-type IX (IXp, A) and X placodes (Xp, B) and more apoptotic cells in *Eya1*$^{-/-}$ IX and X placodes (arrow, C and D). gIX and gX, IXth and Xth cranial ganglia.